

AD-A260 035



2

PL-TR-92-2239

**STUDY OF HIGH SPATIAL RESOLUTION NARROW
SPECTRAL BAND UV IMAGES OF THE
EARTH'S ATMOSPHERE**

John L. Lowrance

**Princeton Scientific Instruments, Inc.
7 Deer Park Drive
Monmouth Junction, NJ 08852**

30 September 1992

**DTIC
ELECTE
DEC 29 1992
S A D**

**Final Report
February 1990-September 1992**

Approved for public release; distribution unlimited



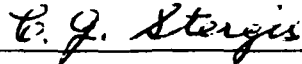
**PHILLIPS LABORATORY
Directorate of Geophysics
AIRFORCE MATERIEL COMMAND
HANSCOM AIR FORCE BASE, MA 01731-5000**

92-32840



92 12 28 015

"This technical report has been reviewed and is approved for publication"



C. G. STERGIS

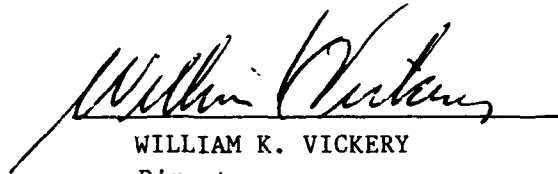
Laboratory Contract Manager



DAVID N. ANDERSON

Chief,

Ionospheric Modelling & Remote Sensing Br.



WILLIAM K. VICKERY

Director,

Ionospheric Effects Division

This report has been reviewed by the ESC Public Affairs Office (PA) and is releasable to the National Technical Information Service (NTIS).

Qualified requestors may obtain additional copies from the Defense Technical Information Center. All others should apply to the National Technical Information Service.

If your address has changed, or if you wish to be removed from the mailing list, or if the addressee is no longer employed by your organization, please notify PL/TSI, Hanscom AFB, MA 01731-5000. This will assist us in maintaining a current mailing list.

Do not return copies of this report unless contractual obligations or notices on a specific document requires that it be returned.

REPORT DOCUMENTATION PAGE

DAIR 100 000 0100

Public reporting burden for this collection of information is estimated to average 1 hour per response, including the time for reviewing instructions, searching existing data sources, gathering and maintaining the data needed, and completing and reviewing the collection of information. Send comments regarding this burden estimate or any other aspect of this collection of information, including suggestions for reducing this burden, to Washington Headquarters Services, Directorate for Information Operations and Reports, 1215 Jefferson Davis Highway, Suite 1204, Arlington, VA 22202-4302, and to the Office of Management and Budget, Paperwork Reduction Project (1010-0188) Washington, DC 20503.

1. AGENCY USE ONLY (Leave blank)		2. REPORT DATE 92/09/30	3. REPORT TYPE AND DATES COVERED FINAL REPORT (February 1990-Sep 1992)	
4. TITLE AND SUBTITLE STUDY OF HIGH SPATIAL RESOLUTION NARROW SPECTRAL BAND ULTRAVIOLET IMAGES OF THE EARTH'S ATMOSPHERE			5. FUNDING NUMBERS PE 62101F PR 4643 TA 11 WUAH CONTRACT F19628-90-C-0052	
6. AUTHOR(S) John L. Lowrance			8. PERFORMING ORGANIZATION REPORT NUMBER PSI-TM-9201	
7. PERFORMING ORGANIZATION NAME(S) AND ADDRESS(ES) Princeton Scientific Instruments, Inc. 7 Deer Park Drive Monmouth Junction NJ 08852			10. SPONSORING/MONITORING AGENCY REPORT NUMBER PL-TR-92-2239	
9. SPONSORING/MONITORING AGENCY NAME(S) AND ADDRESS(ES) Philips Laboratory Hanscom AFB, MA 01731-5000 Contract Manager: Christos Stergis/GPIM				
11. SUPPLEMENTARY NOTES				
12a. DISTRIBUTION/AVAILABILITY STATEMENT Approved for public release; distribution unlimited			12b. DISTRIBUTION CODE	
13. ABSTRACT (Maximum 200 words) The primary objective of this research was development of an ultraviolet sensitive television type camera that would be suitable for use on a polar orbiting satellite to obtain high spatial resolution narrow spectral band images of the earth's atmosphere in the 125 to 320 nm wavelength region. An ultraviolet camera with high spatial resolution was designed for the AURA payload. After the first year, emphasis shifted to ground based UV observations when funding for a space borne UV Imager was not foreseen in the near future. The existing ground based UV Imager was upgraded and used to observe rocket launches and e-beam excitation of the ionosphere. In 1992 a Princeton Scientific Instruments Digital CCD Camera System was modified and used successfully for ionospheric observations as a part of the Combined Release and Radiation Effects (CRRES) program, a multi-instrument program to observe sounding rocket releases of barium into the ionosphere.				
14. SUBJECT TERMS ultraviolet, imaging, ionospheric, CCD			15. NUMBER OF PAGES 32	
			16. PRICE CODE	
17. SECURITY CLASSIFICATION OF REPORT unclassified	18. SECURITY CLASSIFICATION OF THIS PAGE unclassified	19. SECURITY CLASSIFICATION OF ABSTRACT unclassified	20. LIMITATION OF ABSTRACT SAR	

CONTENTS

1.	INTRODUCTION -----	1
2.	IMAGING THE UPPER ATMOSPHERE IN THE 450 TO 900 NM REGION----	2
3.	CCD CAMERA PREPARATIONS FOR CRRES-----	2
4.	THE CRRES OBSERVATIONS FROM ST. CROIX IN JULY 1992-----	4
4.1	BARIUM CLOUD OBSERVING RESULTS-----	4
4.2	RADIO BEAM HEATING OF IONOSPHERE, OBSERVATIONS-----	7
4.3	STAR IMAGING-----	7
5.	ANALYSIS OF GENERAL PROBLEM OF MEASURING THE BRIGHTNESS OF EXTENDED SOURCES AGAINST A BRIGHTER BACKGROUND-----	7
5.1	PIXEL BINNING-----	9
6.	REQUIREMENTS FOR AN OBSERVING CAMERA TO OBSERVE IONOSPHERIC PHENOMENA IN THE VISIBLE AND NEAR INFRARED----	10
7.	ORBITAL HIGH RESOLUTION UV CAMERA-----	11
7.1	PROGRAMMABLE CAMERA-----	12
7.2	CCD-----	13
7.3	SYSTEM DESIGN-----	15
7.4	OPTICAL TELESCOPE DESIGN-----	15
7.5	RELAY OPTICS -----	17
7.6	CAMERA DATA ACQUISITION RATE-----	17
7.7	ON-BOARD DATA STORAGE-----	18
7.8	FILTER WHEEL-----	18
7.9	MCP TUBE/HIGH VOLTAGE POWER SUPPLY-----	18
7.10	CAMERA ELECTRONICS AND MICROCOMPUTER-----	19
7.11	DATA STORAGE/MEMORY BUFFER-----	19
7.12	SOFTWARE-----	19
7.13	GROUND SUPPORT EQUIPMENT-----	19
8.	IN ORBIT CALIBRATION OF AURA SPECTROGRAPHS-----	20
8.1	SUNLIGHT AS A CALIBRATION SOURCE-----	22
8.2	ON BOARD CALIBRATION SOURCES-----	22
9.	LOCKHEED UV CAMERA ASSEMBLY AND THE ALTAIR PROGRAM-----	23
9.1	OPTICS-----	23
9.2	IMAGE SENSOR-----	23
9.3	IMPROVEMENT OPTION NO. 1-----	24
9.4	IMPROVEMENT OPTION NO. 2-----	24
9.5	IMPROVEMENT OPTION NO. 3-----	25
9.6	CONVERTING UVCA TO A SATELLITE PAYLOAD-----	25
9.7	SUMMARY OF UVCA ANALYSIS-----	26
10.	SUMMARY-----	27

Dist	Rev. and/or Special
A-1	

Codes

STUDY OF HIGH SPATIAL RESOLUTION NARROW SPECTRAL BAND ULTRAVIOLET IMAGES OF THE EARTH'S ATMOSPHERE

1.. INTRODUCTION

The primary objective of this BAA contract was the development of an ultraviolet sensitive television type camera that would be suitable for use on a polar orbiting satellite to obtain high spatial resolution narrow spectral band images of the earth's atmosphere in the 125 to 320 nm wavelength region. An ultraviolet camera with high spatial resolution was designed for the AURA payload. The secondary objective of the contract was the improvement and use of UV Imagers developed on previous contracts for making ground-based measurements of the ultraviolet signature of rocket engine exhaust and measurements in the near ultraviolet of the night sky auroral emissions.

After the first year, the emphasis of the contract shifted to ground based UV observations when it became clear that funding for a space borne UV Imager was unlikely to be available to GL in the near future. The existing GL ground based UV Imager was upgraded and used at Vandenberg AFB to observe rocket launches. And later it was taken to Poker Flats, Alaska in the winter of 1991-92 for observations of e-beam excitation of the ionosphere.

The main effort, in 1992 was on modifying Princeton Scientific Instruments Digital CCD Camera System and using it for ionospheric observations as a part of the Combined Release and Radiation Effects (CRRES) program, a multi-instrument program to observe sounding rocket releases of barium into the ionosphere and excitation of the ionosphere by using radio dishes at Arecibo to focus a beam of a high powered radio transmissions on the ionosphere. In late June the CCD camera system was shipped to St. Croix and used during the first two weeks of July to observe sun-lit barium clouds placed in the ionosphere by three sounding rockets. This was a successful observing trip with a number of images of barium clouds acquired during all three sounding rocket launches.

The CRRES program participation and related instrument development will be discussed first in this report because of the current interest and prospects for future research in this area.

2. IMAGING THE UPPER ATMOSPHERE IN THE 450 TO 900 NM REGION

The quantum efficiency of the extended red S-20 photocathode is approximately 4 % at 650 nm. In a microchannel plate intensifier this quantum efficiency is reduced to a detective quantum efficiency, DQE, to about 2% due to the fraction of the photoelectrons that actually enter the microchannels and the gain distribution of the MCP. Gallium Arsenide photocathodes used in Gen III image intensifier tubes have a Qe of about 15 % at 650 nm and a net Qe of no more than 10 % given the MCP input efficiency, etc. The back illuminated CCD with antireflection coating achieves 80% quantum efficiency at 650 nm. This significant higher net quantum efficiency makes the unintensified CCD superior to an intensified CCD if the CCD is cooled to minimize dark current and if the CCD is readout with a low noise video amplifier circuit. Figure 1 is a graph showing the signal-to-noise ratio of these image sensors operating with 650 nm illumination. The photocathode based detectors are assumed to be quantum noise limited and the CCD is assumed to have a readout plus dark current noise of 20 electrons rms per pixel. This is optimistic for the photocathode and realistic for the CCD.

One notes that the CCD is a clear choice over the S-20 at any exposure. It is also better than the GaAs photocathode above signal to noise ratios greater than 3 (peak signal/rms noise).

These graphs assume that the pixel size is the same in all cases. The TEK512 CCD is smaller than the 25 mm photocathode by the ratio of 19/25. So the pixel area of the CCD is 58% of the photocathode pixel of the MCP tubes currently used in the GL UV Imagers. This reduces the advantage of the CCD by this factor but does not change the conclusion that the CCD is a better choice. If the TEK1024 is used, then the CCD pixel is larger by the ratio of 33/25 and the CCD pixel area is 85 % bigger, assuming the same number of pixels across the field of view in both cases. This enhances the CCD's relative performance even further.

3. CCD Camera Preparations for CRRES

The CRRES observations in July 1992 consisted of two separate experiments, one being to obtain photometric images of a barium cloud release from a sounding rocket and the other to observe the atmospheric glow in the ionosphere from focusing a radio beam on the ionosphere. The barium cloud, when illuminated by the dawn sun, was expected to have relatively bright emission centered at 455 nm. The ionospheric emission due to radio beam on the other hand was expected to be as low as ten Rayleighs at 577 and 630 nm, based on earlier experiments.

As discussed in Section 2 of this report, the 455 nm barium and 577 and 650 nm oxygen emission lines anticipated in the CRRES

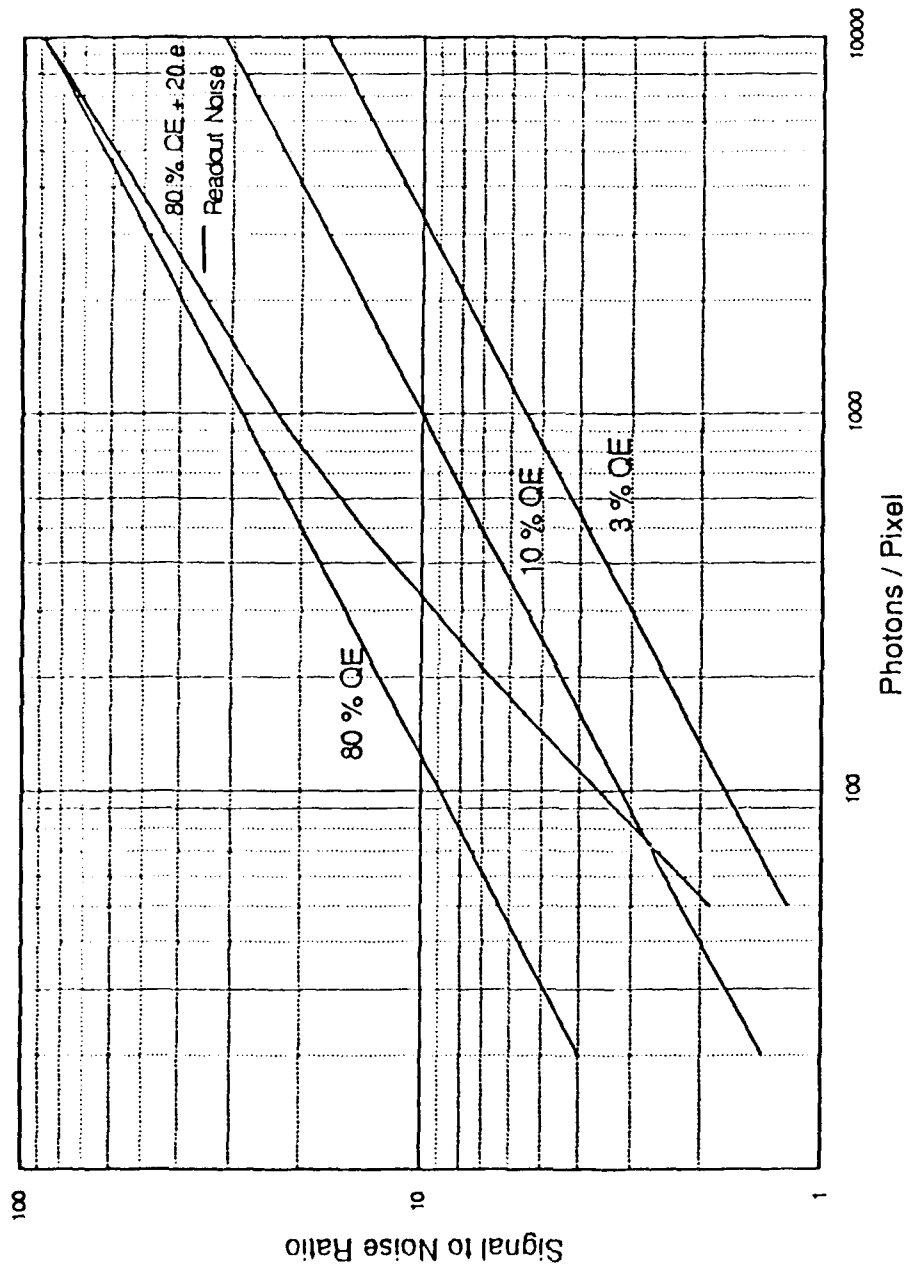


Figure 1: Graph of image sensor peak signal to rms noise ratio versus incident photon exposure in photons per pixel.

observations, made an unintensified back illuminated CCD the preferred image sensor for these observations because of the much higher quantum efficiency of the CCD combined with low readout noise. Such a system would yield substantially better performance over the GL UV Imager system which uses an intensified CCD as a near ultraviolet image sensor. Therefore, for the CRESS measurements, PSI made available, on a loan basis, one of PSI's own Model V CCD cameras which uses an unintensified back illuminated CCD image sensor.

The visible wavelengths of interest for the CRRES observations made it unnecessary to employ the all reflection optics normally used by GL in their ultraviolet imaging, and the low emission brightness of the ionospheric clouds made it important to incorporate into the instrument large aperture optics with a focal length that would have an 8 to 10 degree field of view when combined with the CCD image sensor which was 14 mm square.

Lenses of 4 inch and 8 inch aperture, f/1.38, were designed and built out of Acrylic for these CRRES observations. A housing for the 8 inch lens was designed and built which would fit either the Oriel manual filter wheel on a photometer housing or the PSI 2" filter wheel mounted on the CCD camera.

Two inch optical narrow band filters were acquired from Barr Associates for the 455 and 650 emission lines.

The PSI 2" filter wheel controller was redesigned so that it could be controlled from the microcomputer that controls the Model V CCD camera. Software was written to allow the observer to select a filter exposure sequence and the exposure time for each filter, such that in the observations, the camera would go through a selected sequence and then repeat the sequence.

Software was also written to allow for the continuous transfer of digitized images to memory and to the hard disk of the microcomputer.

A digital tape cassette drive was installed in the microcomputer to allow the digitized observations to be archived on a high density tape to be easily transported.

The liquid nitrogen cooled CCD camera head was adapted to mount the PSI 2" filter wheel with either the 8" or 4" diameter lens and to mount as an assembly on to a heavy duty tripod.

4. THE CRRES OBSERVATIONS FROM ST. CROIX IN JULY 1992

4.1 Barium Cloud Observation Results

In order to minimize the sky background brightness, a narrow band

optical filter centered at 455 nm was used in the CCD camera's filter wheel to image the Barium cloud emission. Since the Barium cloud was sufficiently bright, the CCD camera was run unbinned at 512 x 512 pixel resolution. All observations were done with the CCD camera cooled to a temperature where dark current was negligible in the 30 to 60 sec exposure times employed in these observations.

The coordinates for release of the Barium resulted in a viewing angle from St. Croix observing site of approximately 300 degrees azimuth and 43 degrees elevation. The line of sight range was ~360 kilometers. These numbers varied from rocket launch to launch, but only by a couple of degrees or kilometers. The experiment required that the barium cloud be illuminated by the rising sun while the lower atmosphere was still in the earth's shadow to provide a sufficiently dark background (foreground ?) for viewing the cloud.

Table 1 summarizes the CCD camera observations made from St. Croix.

The first sounding rocket was launched at ~5 AM on July 2, 1992 and the barium cloud was visible through intermittent clouds as a faint blue glow. Fifteen images, each of 60 second exposure, were acquired and recorded with the digital camera.

The second sounding rocket was launched at ~5 AM on July 4, and clear skies allowed more than 40 images to be acquired over a 30 minute period. For these images, movements of the camera tripod during tracking were accurately recorded.

The third sounding rocket was launched at ~5 AM on July 12 and observed for approximately 20 minutes before clouds closed in. Over 22 images were acquired with the digital camera, and again camera tripod movements were recorded during tracking.

These observations of the sunlit ionized barium cloud were successful. The sensitivity of the back illuminated CCD and digital camera system was demonstrated and considerable data was acquired for analysis by Philips Laboratories scientists. Data was transferred to GL by means of a single digital tape holding 100 megabytes of image data.

The experience gained from these first observing trials will be helpful in designing a system specifically for such low luminosity measurements. For example, it would be desirable to have a motorized pointing system, controlled by a joy stick and with automatic recording of azimuth and elevation with each image that is digitized. The ability to change the field of view as the cloud develops and expands was also evident. This can be implemented with a lens turret carrying two or three lenses with differing fields of view or zoom lens system. A larger area CCD would also increase the field of view with the same focal length lens and maintain the sensitivity.

PSI CCD CAMERA		IMAGES COLLECTED AT ST. CROIX			
Date (1992)	Weather	Sky & Flat Field Imaging	Star Imaging	Microwave Heater Imaging	Barium Release Imaging
6/28	Clear	7 Images. Sky Bkgrd.	—	—	—
6/30	Clear, some clouds	Sky Background 9 images 630 & 558 nm 3x bin, 143 sec. exposure	—	9 Images. Heater 5 min. on/off, 630 & 558 nm 3x bin, 143 sec. CCD temp. not constant	—
7/1	Clear, clouds to the west	Sky Background 3 images 630 & 558 nm 3x bin, 144 sec. exposure	—	10 images. Heater on continuously, but frequency not matched to ionosphere. 630 & 558 nm, 3x bin, 144 sec.	—
7/2	Cloudy for Barium release. Clear for background images.	Sky Background 9 images 630, 558 nm 3x bin, 94 sec. exposure	1 image 1 x 1 bin. 299 deg. AZ 42 deg EL	2 images 630, 558 nm 3x bin, 144 sec Heater on continuously	15 images 455 nm filt. 1x bin, 60 sec exp.
7/3	Clear	3 Flat Field Images 455 nm, 1x bin, 60 sec.	3 Images of Vega at 558, 630, & 455 nm 1x bin, 60 sec	—	—
7/4	Clear	5 Flat Field Images 455 nm, 1x bin, 60 sec.	—	—	45 Images 455 nm filt. 1x bin, 30 sec exp.
7/9	Clear	Sky Background 2 images, 630 nm 120 sec. exposure, 3x bin	—	10 images 630 nm 120 sec exp, sky bkgrd. Heater on continuously.	—
7/12	High clouds. Magnitude 2 stars can be seen	Sky Background 5 Images, 455nm, 1x bin 30 sec. Also took Flat Field Images.	—	Heater on for all Images taken on this night	22+ images, 455 nm filt. 1x bin, 30 sec exp.

TABLE 1

4.2 Radio Beam Heating of Ionosphere, Observations

Observing the optical emission resulting from heating by the radar beam was less successful, due to the seeing conditions and the way in which the radar was operated most of the time. To be more specific, the high humidity in the region in July and resulting intermittent cloud cover resulted in fluctuations in the atmospheric transmission that were at least as great as the optical emission in the ionosphere due to the radar beam heating. In an attempt to minimize the uncertainty caused by this varying optical transmission, the radar beam was turned on for 5 minutes and off for 5 minutes. Unfortunately, the atmospheric transmission appeared to change on a shorter time scale than 5 minutes so that this was not effective. In addition, modulating the beam in this manner seemed to be difficult and was discontinued early in the series.

From the experience gained from this campaign, one concludes that accurate observation of radio beam heating phenomena would be greatly improved by making the observations above the fluctuating atmosphere from an airborne platform such as a high flying airplane, above the clouds and high humidity atmosphere.

One possibility of making useful radio beam heating observations from the ground may be to chop the radar beam on and off at a frequency that would eliminate the fluctuations due to the changing optical transmission along the line-of-sight, and then integrating the individual measurements over a long enough time base to improve the quantum noise limited signal-to-noise ratio.

4.3 Star Imaging

In the course of calibrating both the CCD camera and the tripod azimuth and elevation controls several star images were taken. On one of the relatively clear nights, 3 pictures of Vega were taken at each of the 3 filter positions (455, 558, and 630 nm). The angular size of a pixel in the image plane is $27/140,000 = 0.0002$ radian = 3.98 arc seconds. Since there was no sidereal drive on the camera mount-tripod, and the sidereal rate is 15 arc seconds per second, the effective exposure time for a star was only 3.8 seconds/pixel. This was the time it took for a star to travel across a given pixel width. On examining the images it was agreed that 6th magnitude stars could be detected, which is respectable performance considering the observing conditions, the 4 inch collecting aperture, and the inability to truly integrate the star light due to the lack of a sidereal drive on the tripod.

5. ANALYSIS OF THE GENERAL PROBLEM OF MEASURING THE BRIGHTNESS OF A FAINT EXTENDED SOURCE AGAINST A BRIGHTER BACKGROUND

In attempting to measure the brightness of an extended source against a brighter background, one is limited by the statistical

"quantum noise" associated with the background. For example, the rms noise in the background is equal to the square root of the number of photoelectrons detected in the measurement, i.e. the number of photoelectrons per pixel in the exposure. The object of interest must generate a signal, again in photoelectrons per pixel, that is measurably larger than this noise in the background. For example, a background of 10,000 photoelectrons per pixel has a quantum noise of 100 photoelectrons. This fundamental limit on the measurement is illustrated in more detail in Table 2, using parameters relevant to the instrument and measurement conditions relevant to CRRES.

CCD pixel size = 27 microns
 Focal Length = 140 mm
 Aperture Dia. = d = 100 mm
 Altitude = H = 300 km
 Pixel at Alt = a = 60 meters
 Pixel in radian = $60/300,000 = 1/5,000$ radian
 Estimated atmospheric attenuation = 0.5
 Filter transmission = 0.6
 Optical " = 0.8
 Net Optical Eff. = E = 0.25
 Quantum Efficiency = 0.66 (typical back illuminated Tektronix CCD)

$$\text{Exposure} = \text{REt} \left(\frac{a d}{H} \right) 8 \times 10^8 \text{ photons/pixel/sec/Rayleigh}$$

Exposure = 0.06 R t for the above set of parameters.

For $Q_e = 0.66$ photoelectrons per photon

$$\text{Exposure} = 0.04 R t \text{ photoelectrons/pixel/sec/R}$$

The transfer function of the digital CCD camera is 1 ADU = 6.4 microvolt. The CCD on chip amplifier has a transfer function of ~0.64 microvolt per photoelectron. Thus 1 ADU = 10 photoelectrons.

It works out that for an exposure time of 140 seconds and pixel binning factor of 3 x 3, Exposure = 77 photons/pixel/R

and the overall camera system transfer function becomes 5 ADU per Rayleigh for this 140 second exposure and 3x pixel binning.

These equations are expressed in tabular form in the following table for a range of backgrounds measured in Rayleighs.

TABLE 2

R	t	Qe	pe/pix	bin 3x3	rms noise,pe	%	rms noise,R
2500	143	0.66	14,157	127,413	357 pe	0.29	7.0 R
2000			11,326	101,934	319		6.27
1500			8,494	76,446	276		5.44
1000			5,663	50,967	225		4.44
500			2,831	25,479	160		3.13
250			1,416	12,741	113		2.22

One notes that a 500 R background results in 25,479 photoelectrons with a square root of 160 electrons = rms quantum noise = 0.6 % = $500 \times 0.006 = 3.13$ R rms. Decreasing the exposure time by a factor of 9 to 16 seconds, increases the noise to 9.38 R, a factor of 3 corresponding to the factor of 9 decrease in the number of photoelectrons per pixel. This is the tradeoff between temporal resolution and background noise. Decreasing the binning from 3x to 1x results in a corresponding factor of 9 decrease in the number of photoelectrons per pixel and the same factor of 3 increase in background noise. In this case the pixel size changes from 180 to 60 meters square, so there is a tradeoff between spatial resolution and background noise.

The noise tabulated in Table 2 is the best that one can do, based on the physics of the problem. Other noise sources and inefficiencies will increase the background noise over what is shown in Table 2.

The situation can be improved by increasing the number of photoelectrons per pixel. This can be done by employing a larger optical aperture. Since there is a limit in the focal length to diameter ratio at about f/1 the only way to increase the diameter is to also increase the focal length of the optical system. For a given field of view, the image sensor must increase in proportion to the increase in the focal length and aperture diameter. In the instrument used for the July 92 CRRES measurements, the image sensor was $512 \times 0.027 = 13.824$ mm square. Increasing the optical aperture to 200 mm would require doubling the linear dimension of the image sensor in order to maintain the 5.6×5.6 degree field of view. In return the noise would be reduced by a factor of 2 over the values listed in Table 2. Larger area CCD image sensors are commercially available.

5.1 Pixel Binning

The CCD can be operated in a way that allows the pixels to be summed vertically and horizontally prior to readout via its on-chip

amplifier. This binning process involves adding the photoelectron charge accumulated in individual pixels (#pe) together in the readout process and generates negligible additional noise. On chip binning does require a digital camera with microcomputer control of the CCD readout process. It cannot be implemented on the analog CCD cameras currently used in the UV Imager. PSI designs and sells such digital CCD cameras for scientific applications.

This facility to bin pixels allows the size of the focal plane pixel to be selected for a particular observation to maximize the signal-to-noise ratio as a trade-off against spatial resolution, at a given optical focal length. The signal-to-noise ratio in a binned pixel is expressed in the following equation:

$$\frac{\text{Peak Signal}}{\text{RMS Noise}} = \frac{(\#pe/\text{pixel}, N) (\text{Binning Factor}, B)}{[NB + I_d B + R_n^2]^{1/2}}$$

where I_d is the dark current per pixel and R_n is the rms readout noise per pixel in electrons.

This points up the need for lower dark current in the binned mode in order to take maximum advantage of binning to improve the signal to noise ratio, i.e. $I_d B$ should be $< R_n^2$.

6. REQUIREMENTS FOR AN OBSERVING CAMERA TO OBSERVE IONOSPHERIC PHENOMENA IN THE VISIBLE AND NEAR INFRARED

The recent CRRES observation experience from St. Croix and the above analysis of the observing situation provide a sound basis for designing a camera specifically for collecting photometric data on such low luminosity extended source phenomena in the ionosphere.

The primary consideration is object brightness levels as low as ~10 Rayleighs. This, in turn requires that the background be made low as possible by narrowing the optical bandwidth to match the spectral bandwidth of the emission of interest, and to pick an observing site that has intrinsically low background. On this point, the northern latitudes are hampered by natural aurora and at the southern latitudes, there is the problem of clouds and in the case of St. Croix ambient street lighting from the inhabited island. The best solution to this problem is to configure the camera so that it can be located in an airplane as well as used from the ground. This requirement is not difficult to meet, but does place constraints on the means for cooling the image sensor.

Camera Design Requirements:

The image sensor should be cooled to minimize dark current background and the cooling should be thermoelectric or some closed cycle refrigeration system.

The cooled camera head and electronics should be packaged to fit into an airplane as well as on a ground based mount.

The camera mount should have joy stick type pointing controls so that an operator looking at the television image from the camera can point the camera remotely.

The camera should be digital in order to minimize the data recording noise and preserve the dynamic range. Twelve to sixteen bit digitization is recommended.

The camera image sensor should have as large an image area as possible in order to maximize the light collected at a given field of view.

The camera controls should provide software-keyboard selection of the pixel size and integration time as well as filter wheel control

The quantum efficiency of the image sensor should be as high as is available at the wavelengths of interest. The signal capacity of the image sensor should be large enough to meet the criteria indicated in Table 2 for detecting ionospheric emission of interest against a significantly brighter background.

7. ORBITAL HIGH RESOLUTION UV CAMERA

The objective was to design and build an ultraviolet sensitive television type camera for use on a polar orbiting STEP satellite to obtain high spatial resolution narrow spectral band images of the earth's atmosphere in the 125 to 320 nm wavelength region. The general requirements for the high resolution imager were the following.

Day and nighttime modes of operation, programmable from the ground several days in advance.

Pixel binning from 1 to 16 pixels in each dimension, programmable from ground.

12 bit video A/D with ground control of which bits and how many bits are actually transmitted.

Time delay integration capability but do not include yaw

correction.

Programmable 6 position optical filter wheel with narrow band UV filters.

Use frame transfer CCD with storage register to facilitate programmable electronic shuttering of camera exposure time.

Portable ground support equipment (GSE) equipment that can program camera and display camera output.

Camera Parameters

Spatial resolution-----	100 meters per CCD pixel
Swath width-----	50,000 meters
Spectral range-----	1250 to 3200 Angstroms
Spectral Resolution-----	200 Angstroms
Exposure, 2000-3200 A, day mode---	1 kR/A, continuum spectrum,
Exposure, 1250-2000 A region, day mode---	1 R/A with 10x binning,
narrow emission lines averaging out to 1 kR over 200 A band	
Intra-scene dynamic range-----	100 to 1
Orbit Altitude-----	1000 km
Orbit -----	polar
Image Diagonal	25 mm
Frame Rate	variable
Data Rate	20 kBits/sec (orbit average)
Photocathode	CsTe
Window Material	MgF2
Mission Life	0.5 to 3 years

The proposed operating flexibility of the AURA camera made it distinctive from other proposed UV imaging experiments.

One interesting possibility would be to use a 1000x500 pixel CCD, This would allow higher spatial resolution (50 m) in the 2000-3200 band when gathering UV clutter background data. This CCD would have an equal size frame transfer storage area. The image would have 8 times the number of pixels of the MSX imager.

7.1 PROGRAMMABLE CAMERA

It is clear that the camera needs to be programmable via ground commands to the satellite and that these programs and associated camera modes are complicated enough that a microcomputer embedded in the camera electronics is the best way to provide this capability. The camera will have the following programmable features and functions.

a. programmable exposure time

- b. programmable time delay integration (TDI)
- c. video gain, 2 selectable gains
- d. pixel binning in x and y, selectable from 1 to 16 pixels.
- e. programmable filter selection
- f. adjustment of CCD operating voltages via telemetry link
- g. programmable sequence of camera modes to accommodate day night operation, etc.

7.2 CCD

The CCD needs to be a frame transfer type in order to accommodate electronic shuttering and programmable time delay integration modes of operation.

Large pixels reduce demagnification between the phosphor screen and CCD. The optical coupling loss between the image tube phosphor and CCD goes as the square of the magnification.

The following table lists some of the CCD choices:

TABLE 3

Type	Pixel size	Format	Image width
Thomson CSF	23 micron sq.	288V x 384H	8.83 mm
EEV	22 micron sq.	288V x 385H	8.47 mm
EEV	22.5 micron sq.	576V x 298H	6.7 mm
TI	22.4 micron sq.	288V x 390H	8.74 mm
TEKTRONIX	24 micron sq.	512V x 1024H	24.6 mm

Each of these CCDs has a frame storage register equal in size to the image format.

The typical dark current of candidate CCD's is listed below for 20 degrees Celsius.

Tektronix-----	3,000 electrons/pixel/second
EEV-----	50,000 "
ThomsonCSF-----	50,000 "
TI-----	12,000 "

In the time delay integration mode, the CCD line rate is equal to

the ground pixel rate. As discussed elsewhere, the CCD pixel is approximately 70 meters. The 750 km orbit satellite's ground track velocity is approximately 6.65 km per second. The readout rate is then $6,650/70 = 95$ lines per second. For a CCD having 288 vertical pixels (288 horizontal lines) the frame period is approximately 3 seconds. However, the frame transfer type CCD has a storage register that is of equal size such that the pixel actually traverses $2 \times 288 = 576$ pixels and would take 6 seconds. During this 6 seconds the pixel accumulates dark current which adds to the signal.

In the normal mode of operation, the exposure time can be considerably shorter, depending on the optical exposure time and the pixel binning factor. This is shown in Table 4.

TABLE 4

Binning Factor	Optical Exposure	Readout Time	Total Time	Dark Current X Factor
1x1	0.015 sec	3.00 sec	3.0 sec	3
2x2	0.03	0.75	0.8	3.2
3x3	0.045	0.33	0.4	3.6
4x4	0.06	0.19	0.3	4.8
5x5	0.075	0.12	0.2	5
10x10	0.15	0.03	0.2	20
30x30	0.45	0.003	0.5	450

This table is based on somewhat idealized analysis but the total dark current accumulation time is about right. The macro-pixel dark current factor is tabulated for various binning factors.

Referring back to the room temperature dark current for the Tektronix CCD of 3,000 electrons per sec per pixel, a 10x10 binning factor would result in $20 \times 3,000 = 60,000$ electrons dark current per macro-pixel.

The rms random noise associated with this dark current is 245 electrons, equal to the square root of the number of dark current electrons, (60,000). Assuming that the image intensifier and optical coupling to the CCD and CCD quantum efficiency has a net gain of 50 CCD electrons per photoelectron, this CCD dark current related noise, referred to the photocathode, is divided by this factor, $245/50 = 5$ photoelectrons dark current noise per macro pixel. This is quite tolerable, suggesting that the Tektronix CCD could be used uncooled. Unfortunately Tektronix does not currently make a 288 line frame transfer CCD. The TEK 512x1024 CCD could be binned 2x2 to yield a 256x512 format. The dark current would increase by 4x and dark current noise would become 10 photoelectrons per pixel, still an acceptable value.

The TI CCD dark current is a factor of 4 greater than the Tektronix

CCD, but the same as the 2x2 binned Tektronix chip. So the dark current noise would be the same in comparable formats.

The CCD dynamic range is reduced by this same gain factor of 50, resulting in a maximum signal in this case of $500,000/50 = 10,000$ photoelectrons per pixel. This is more than adequate and suggests that higher gain may be desirable. This is possible by increasing the image intensifier gain or by going to fiber optic coupling between the image tube and CCD.

From this analysis it appears that moderate cooling is needed in order to use the EEV and Thomson-CSF CCDs, and substantial cooling will be required with macro-pixels larger than 10x10. Passive cooling may be possible, depending on the spacecraft configuration. Further analysis of this point must await data on the spacecraft.

The proposed system is based on employing only passive cooling as needed for the CCD. The actual CCD choice will be made in the design phase once the system tradeoffs can be made.

7.3 SYSTEM DESIGN

Configuration

Figure 2 is a block diagram of the envisaged AURA camera. A microcomputer is an integral part of the camera system serving to change the operating modes of the camera under ground command and to manage the data acquisition. A 15 million bite digital memory is shown as the means of storing images collected over regions of interest such as the poles and transmitted to the ground when passing over a ground station. If the spacecraft can provide this data storage, a smaller memory can be used as a buffer to the spacecraft.

7.4 OPTICAL TELESCOPE DESIGN

Taking the TI CCD format width of approximately 390 pixels and a digital sampling factor 1.4 times the spatial resolution of interest, the number of cross track pixels becomes $390/1.4 = 278$. The cross track width is then $278 \times 100 = 27.8$ km. At 1000 km this corresponds to an angle of 1.6 degrees and a diagonal of 2 degrees, (3x4 aspect ratio).

This angular field of view can most probably be provided by a two mirror telescope, perhaps with some field flattening provided by figuring the input window of the image tube.

The 3x4 aspect ratio of the image format on a 40 mm diameter image tube results in a horizontal width of 32 mm and $32,000/278 = 115$ micron wide pixels (4.3 lp/mm). The 100 meter pixel subtends

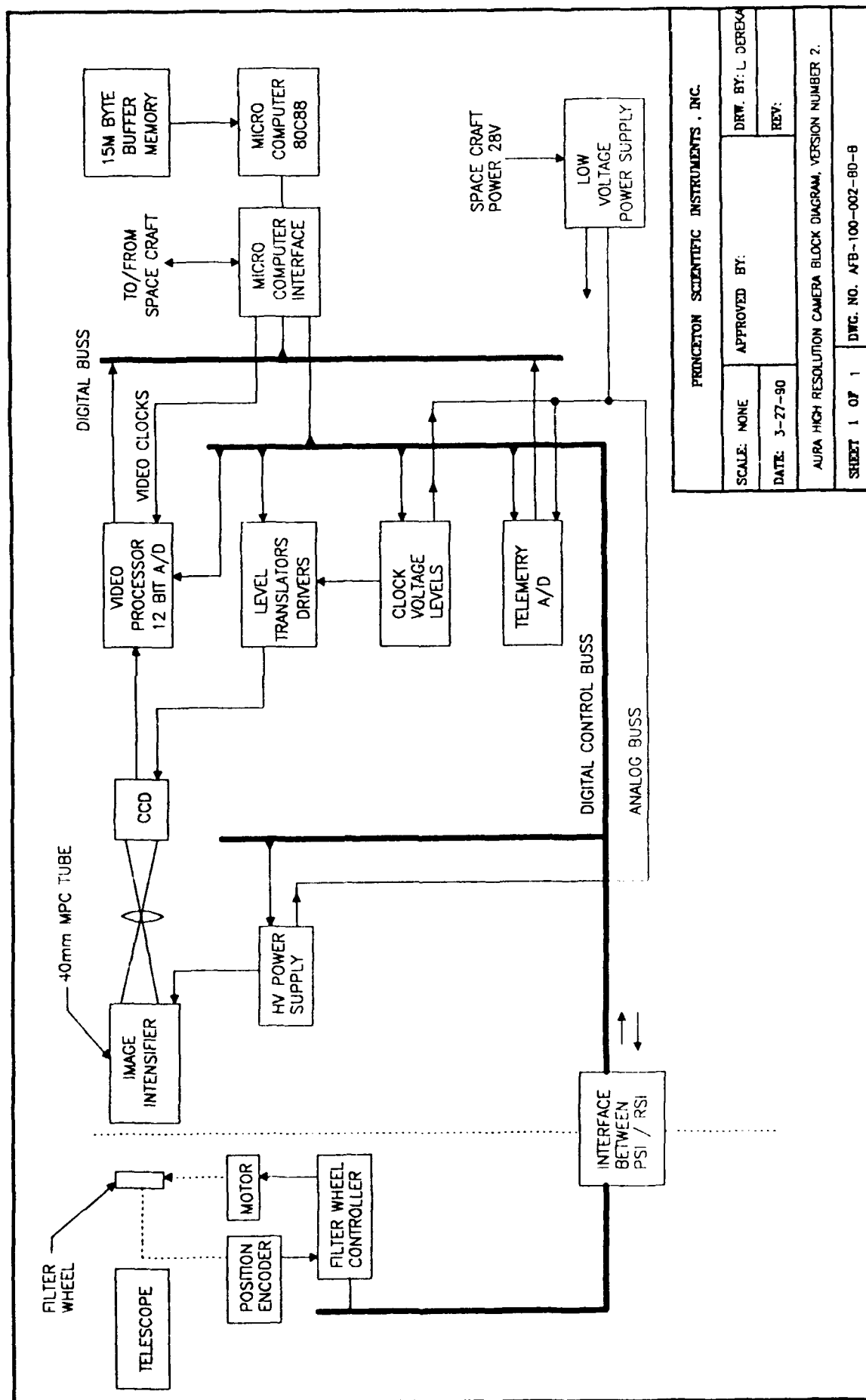


FIGURE 2

10E-4 radian at 1000 km resulting in a telescope focal length of 1000 mm. And with a 200 mm aperture, the focal ratio becomes f/5. For a 25 mm diameter image tube format, the pixel size is 25/40 times as large resulting in 73 micron pixels (6.8 lp/mm), a 625 mm focal length and f/3.1. The optical performance of a Cassegrain type telescope may not be adequate at a fast focal ratio of f/3.1.

The image tube's MTF in the ultraviolet at 4.3 lp/mm is about 65%, and at 6.8 lp/mm the MTF is about 30%. This 50% loss in MTF with the 25 mm tube is a tradeoff against a small and therefore lighter filter wheel. The weight of the telescope and other system components remain about the same in either case. The MTF of the telescope is also improved at f/5 compared to f/3.1. The proposed camera is based on a 40 mm tube.

Preliminary optical designs indicate that the optical performance needed for the camera can be met with a Ritchey-Chretien type two mirror telescope, 200 mm in diameter and 1 meter focal length with a focal plane 40 mm in diameter. The focal plane curvature may require figuring the faceplate of the image tube. There is no off the shelf telescope that meets the requirements for this space application.

7.5 RELAY OPTICS

The optical demagnification between the 40 mm image tube and CCD is $32/8.8=3.6$. The magnification in the case of a 25 mm tube is 2.25 to 1. Assuming the same focal ratio optics, the optical coupling efficiency is 2.56 times greater in the case of the 25 mm tube. Whether this is important or not depends on the gain of the image tube to begin with, i.e. one wants the system noise to be quantum noise limited. This means that the signal from one photoelectron should be comparable to or larger than the system noise, in this case the CCD readout noise. In lens coupling, the distance between the object and image planes is related to the magnification also. $1/a + 1/b = 1/f$ and the magnification $m=a/b$. Assuming the 17 mm lens used in ground based UV imagers, the optical path length is 20 mm longer for the 40 mm format compared to the 25 mm format.

7.6 CAMERA DATA ACQUISITION RATE

The satellite velocity is approximately 6.65 km/sec corresponding to 66.5 hundred meter pixels per second in the satellite orbital track direction. With 390 digital pixels per line this becomes $66.5 \times 390 = 25,935$ pixels per second referred to the object plane. In order to minimize the $\sin x/x$ filtering and aliasing associated with the quantizing and digitizing process, the same digital sampling factor 1.4 times the ground resolution of interest is applied in the vertical direction also. The digitized pixel rate would be approximately 36,000 pixels per second and at 12 bits per

pixel, 435,000 bits per second. This is the average pixel rate for contiguous coverage along the satellite ground track. Overlapping images can be acquired by increasing the readout rate and would increase the average data rate. The data rate can be reduced by skipping along the ground track.

Binning pixels together reduces the data rate correspondingly. For example a binning factor of 2x2 would reduce the data rate to 9,000 pixels per second.

7.7 ON-BOARD DATA STORAGE

20,000 bits/sec corresponds to 1,600 twelve bit pixels per second. Assuming an orbit period of 105 minutes, the total orbit data dump would be 10 million pixels. This corresponds to 40,000 lines of 250 pixels each. And at 100 meter resolution this is a swath 50 km wide and 2,000 km long. This is assuming that the imager takes all of the data, which would not normally be the case.

Assuming that the orbital transmission limited maximum of 10 million pixels is acquired over the poles away from a ground station, the on board memory needs to be 15 million bites, shared by the spectrograph and high resolution camera. It is understood that the spacecraft will have on board data storage.

It is envisaged that the AURA camera and spectrographs will have a buffer memory with a capacity of approximately 2 megabytes. This buffer will allow the readout rate of the camera and spectrograph to be decoupled from the data rate of the spacecraft data storage system. The buffer memory is based on using a commercially available memory board that is engineered to work with the camera's microcomputer.

7.8 FILTER WHEEL

A six position filter wheel has 5 positions for 2 inch diameter filters and one blank position for mechanically shuttering the system. The filters should be solar blind with approximately 20 nm bandpass.

7.9 MCP TUBE/HIGH VOLTAGE POWER SUPPLY

The MPC intensifier tube can be a standard ITT 40 mm tube with MgF2 window and CsTe photocathode. The tube should be burned in for 48 hours to check for photocathode stability. It may be necessary to figure the window to give it some optical power in order to act as a field flattener for the telescope.

The MCP tube requires approximately 6,000 volts between the MCP and the phosphor, 800 volts across MCP, and 180 volts between photocathode and MCP.

7.10 CAMERA ELECTRONICS AND MICROCOMPUTER

Figure 2 is a block diagram of the camera system. The camera electronics design and fabrication will be done by PSI using the experience from building similar CCD cameras for ground based astronomical CCD cameras and ongoing UV imaging system research currently supported by GL. The design will use space qualified components where possible. The microcomputer for the electronics will be selected for the space radiation environment. The microcomputer used in the STEP spacecraft will be considered for use in the camera. The budget assumes that a low power CMOS type off the shelf microcomputer can be obtained and with minor modification, work reliably in the AURA satellite mission.

7.11 DATA STORAGE/MEMORY BUFFER

It is understood that satellite would have ~ 200 MB digital tape recorder and that this tape recorder is sized to hold 3 orbits worth of data from up to 4 instruments. This translates into about 16 MB per orbit for the AURA instruments. The plan is for AURA to have a 2 MB buffer memory that can take in data from the HR camera and the spectrographs and then dump batches of data to the tape recorder for later transmission to the ground station.

This proposal is based on using low power CMOS memory board that are commercially available and heat sinking these boards to take the vacuum thermal environment.

7.12 SOFTWARE

The microcomputer controlled camera and data storage subsystem will require specific software development to control the system and handle commands from the spacecraft and to transfer data to the spacecraft for transmission to ground. This software development is a part of the camera system proposal.

7.13 GROUND SUPPORT EQUIPMENT

The Ground Support Equipment for the AURA HR camera is based on a microcomputer based data acquisition system. Software will be written to simulate the spacecraft interface and to acquire and display camera data. This GSE will also be made air freight transportable so that it could be set up at a ground station to display camera data received by the ground station. This will be invaluable in evaluating the system performance in orbit.

8. IN ORBIT CALIBRATION OF AURA SPECTROGRAPHS

There is a need to calibrate the ultraviolet spectrographs in orbit that are a part of the new AURA payload. The following is an analysis based on using ultraviolet stars for this purpose.

AURA Specifications

Slit Field of View--0.058 x 1.45 degrees

Optical Band of Interest--1150 to 1700 Angstroms

Slit Image corresponds to 5 Angstroms

Optical Aperture 49 x 63 mm = 3089 sq. mm.

Optical Efficiency, Including Spectrograph_____ 25% ?

Photomultiplier Quantum Efficiency---15%

Exposure Time----- The orbit period is approximately 100 minutes or 6000 seconds of time. The angular rate is 360 degrees in 6000 seconds or 0.06 degrees per second. Therefore a star would cross the slit in 1 second of time and traverse the length of the slit in 24 seconds.

It is preferable to do the calibration in the dark portion of the orbit which is perhaps 40% of the orbit period. Therefore the dark angle swept by a slit aligned normal to the velocity vector is

$$1.45 \times 0.4 \times 360 = 209 \text{ square degrees per orbit.}$$

If the slit is aligned along the velocity vector then the dark angle swept by the slit is $0.058 \times 0.4 \times 360 = 8.35$ square degrees per orbit

Referring to Figure 3, Star Distribution, from Star Trackers and Systems Design by Quasius and McCandless, there would be at least one star +6 visual magnitude or brighter in 8.35 square degrees.

A zero magnitude star has a brightness of approximately 1000 photons per second per Angstrom per square centimeter of collecting aperture. +6 magnitude corresponds to an attenuation of $2.5E6$ or a factor of 250. Therefore, the signal collected by the 30 cm aperture would be

$$(1000/250) \times 30 \text{ cm} \times 0.15 \times 0.25 \times 5 \text{ A} = 23 \text{ photoelectrons per second}$$

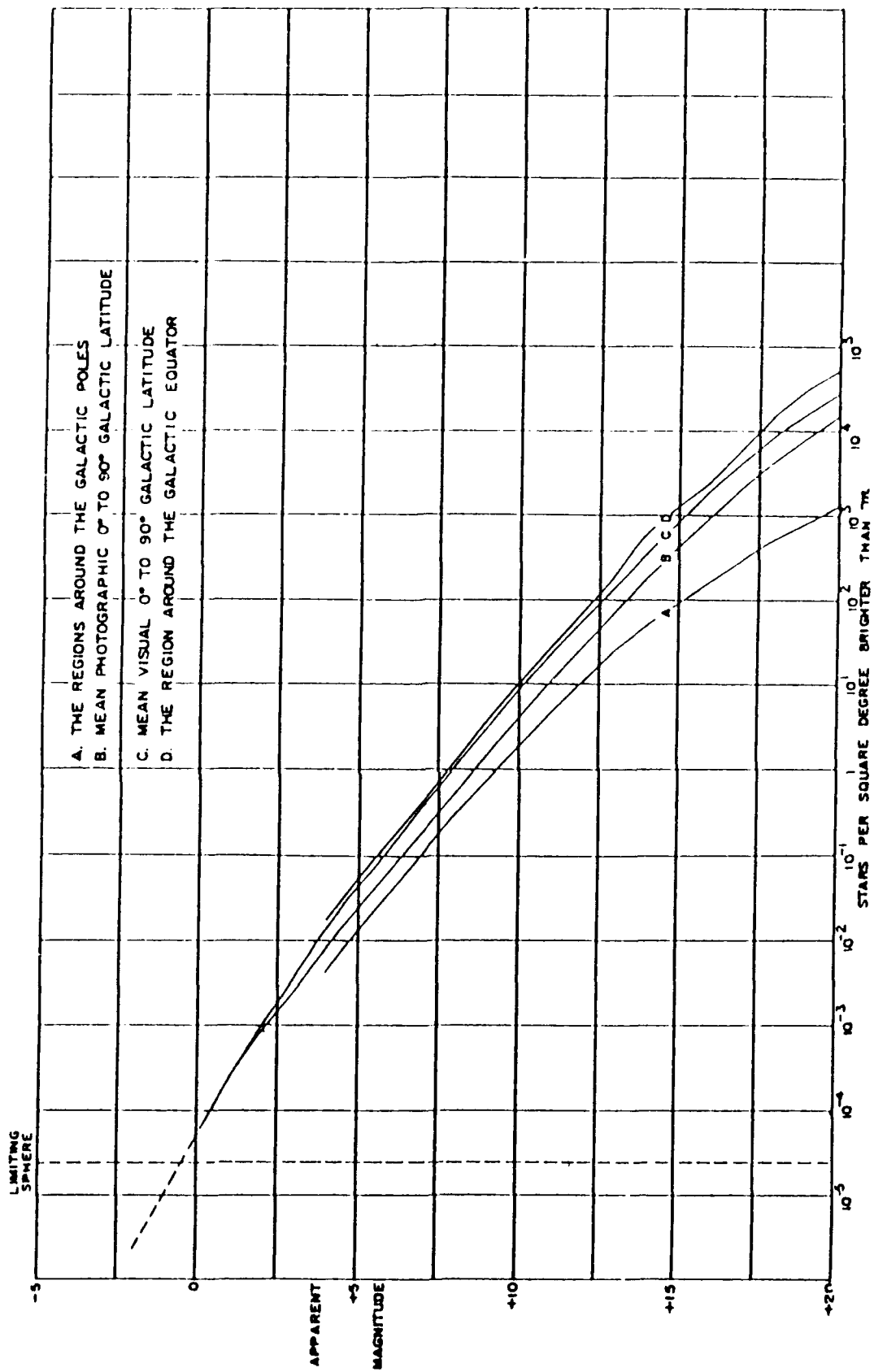


FIGURE 3

This analysis is related primarily to visible light, not the ultraviolet. There are fewer stars that are bright in the ultraviolet and the brightness in the 1150 to 1700 Å band is also typically lower, so, on the average the signal from a star would be at least an order of magnitude less, say 2 photoelectrons per second. In the optimistic case where the star stayed in the slit over its 1.45 degree length the exposure time would be 24 seconds and the total signal would be approximately 50 counts with a corresponding quantum noise limited S/N of 7. Thus, one 5-Ångström point would be calibrated per orbit to a maximum accuracy of 14%, presuming the star can be identified and its ultraviolet flux is known or if the same star can be acquired from time to time and can be known to be the same star.

Next, consider the case where the slit is normal to the velocity vector. In this case the field per orbit is approximately 200 sq. degrees and it is probable that at least one 4th magnitude star will cross the slit. The star would be ~7x brighter but the dwell time in the slit is reduced by about the same factor so the net result is the same as with the slit oriented along the direction of travel. One should also note that only one 5-Ångström point on the calibration curve would be calibrated in a given star encounter.

From this admittedly cursory analysis, one concludes that the stars cannot be used for calibration of AURA spectrographs.

8.1 SUNLIGHT AS A CALIBRATION SOURCE

During the sunlit portion of the orbit there may be enough light scattered by the spacecraft and payload to generate a background signal which is relatively constant from orbit to orbit. It may be possible to increase the scattered light entering the instrument by positioning the scanning mirror to include in its field of view a small solar reflector. This reflector must, of course be made in a way that it does not deteriorate with long exposure to the sun. Perhaps Gold and Platinum or diamond film should be considered. One significant advantage of this scheme is that the sun spectrum is well known and the spectrum could be scanned by AURA in a short time.

8.2 ON BOARD CALIBRATION SOURCES

Calibration lamps are of course a possibility but one wonders how the lamp is ageing. One might also consider a Cerenkov radiation source using an on board radiation source or passes through the South Atlantic Anomaly. In considering such an on board calibration source, one must solve the problem of including the scanning mirror in the optical path since it may change with time also.

9. LOCKHEED UV CAMERA ASSEMBLY AND THE ALTAIR PROGRAM

Lockheed built a UV camera assembly UVCA for use as a Shuttle Payload. This mission was subsequently canceled and the payload was available to the Philips Laboratory for use on a new unmanned satellite ALTAIR.

The following is an analysis as to how the Lockheed UV Camera Assembly's (UVCA) spatial resolution could be improved to the point that there is significant spatial frequency response at 10 micro-radian angular resolution.

The following is a summary of the UVCA parameters as currently configured, based on the 1987 viewgraphs and a telephone call to Stephen Mende, Principal Investigator at Lockheed on the UVCA.

9.1 OPTICS

Cassigrain Telescope

Focal length-----	5,100 mm
Focal ratio-----	f/25
Field of View-----	3.9 x 2.5 milliradian
Focal Plane Scale----	196 microradians per mm
10 micro-radian -----	50 microns in focal plane
	10 cycles/mm spatial frequency
Image Raster-----	380 x 290, 10 x 12 microradian pixels,
	19.4 x 12.3 mm format, (24.5 mm diagonal)

The analog video output of the CCD camera was to be recorded on the Shuttle's standard television format video recorders.

9.2 IMAGE SENSOR

The image sensor consists of two proximity focused micro channel plate image intensifiers fiberoptically coupled together and coupled to a CCD via tapered (1.7 to 1) fiber optics. The CCD is a Fairchild interline transfer CCD with 488 x 380 pixels binned by two vertically to provide pixels on 30 micron horizontal centers and 36 micron vertical centers. With the 1.7 taper the CCD pixels correspond to 50 x 60 microns in the telescope focal plane.

There is no information on the spatial frequency response (MTF) of the individual UVCA components. Mende reports that "most of the image of a point source falls within 3 pixels (30 microradians), as measured with the completed camera".

I have made the following estimates of the component MTFs to get a feel for how the spatial resolution might be improved.

ITEM	f/25 UVCA MTF@10 c/mm	f/40 UVCA MTF@6 C/MM
Pointing Smear	0.8	0.8
Telescope Optics	0.8	0.9
UV MCP Tube	0.2--0.3?	0.5
Visible MCP Tube	0.6	0.8
Fiber Optic Reducer	0.5--0.8?	0.8
CCD	0.5	0.5
Net MTF	0.02-0.05	0.12

9.3 IMPROVEMENT OPTION #1

The f/40, 6 c/mm column is based on changing from a 25 mm to 40 mm diameter image tubes. The optical focal length is increased by 40/25 and the optical filter diameters from 25 to 40 mm. The fiber optic focal reducer would have a reduction ratio of 2.7 rather than 1.7. The result is a significant improvement in MTF but still results in a marginal instrument for resolving 10 microradian features.

Please remember that the MTFs listed are educated guesses. Actual MTF data should be obtained from Lockheed if available.

9.4 IMPROVEMENT OPTION #2

The MTF of the CCD can be improved by using a CCD having more pixels. The CCD MTF, to the first order, is characterized by the function $\sin x/x$. And at the spatial frequency where two pixels equal one cycle the function has a value of about 60%.

Reducing the number of serial components in the camera would also improve the MTF. The minimum components would be to have the telescope, filter wheel and an ultraviolet sensitive CCD. There are CCDs, coated with a fluorescent phosphor that acts as a wavelength converter, converting the short wavelength photons to longer wavelengths where the silicon CCD is sensitive. (1) In the proposed application, however, the target flux levels may be too low to overcome the CCD readout noise. This can be overcome to some extent by reducing the camera frame rate from 60 frames per second to perhaps 1 frame per second.

Following this approach the telescope focal length and focal ratio could remain at f/25 with the following result.

ITEM	MTF at 10 c/mm
Pointing	0.8
Telescope	0.8
CCD	0.5
Net MTF	0.3

One could consider using a CCD with twice the number of pixels per line, with the option of "binning pixels together" prior to readout as a means of reducing readout noise when the exposure level is very low. At exposure levels where there is sufficient light the unbinned CCD MTF would provide an MTF at 10 c/mm of about 70% with a net MTF of about 45%.

This scheme is attractive from the spatial resolution standpoint. It does give up temporal resolution. It also imposes greater demands on the optical filters which have to do a better job of excluding long wavelength light since the CCD has high Qe out to about 9000 Angstroms.

9.5 IMPROVEMENT OPTION #3

The two MCP type image intensifiers, fiber optic taper and CCD camera could be replaced by an electron bombarded CCD camera. In this case photoelectrons emitted from a solar blind photocathode are accelerated and strike the silicon CCD. The energy of the accelerated photoelectron is converted into signal electrons in the CCD at a conversion factor of one signal electron per 3.6 eV. The typical gain is several thousand comparable to the net gain of the two stage MCP tubes fiber optically coupled to the CCD. The advantage of this approach is that the MTF of the single electron bombarded CCD image tube can be significantly higher than the existing image tube/CCD combination. Tubes of this type have been made and used but are not commercially available. I had such tubes made by Varian and later RCA for use in nuclear fusion research at PPPL.

The net MTF would be about 0.4 with the advantage of being solar blind and the temporal response would not be restricted by low flux levels.

It would be possible to do "photon counting with this image sensor, provided one wanted to add the necessary digital memory to the payload. It should be noted, however, that photon counting would not be possible or necessary at high flux levels.

9.6 CONVERTING UVCA TO A SATELLITE PAYLOAD

In addition to improving the spatial resolution, the UVCA must be modified in other ways for use by the ALTAIR satellite. For example

the analog video must be digitized and stored on the satellite for subsequent transmission to a ground station or to a data relay satellite. The command and control telemetry interface to UVCA is currently designed for the Shuttle and semi-manual operation. This must be modified for ALTAIR.

The 60 frame per second operation is an outgrowth of the Shuttle and its standard television video tape recorders. The frame rate needs to be assessed based on the satellite mission and the science requirements.

9.7 SUMMARY OF UVCA ANALYSIS

The UVCA spatial resolution can clearly be improved. I will be happy to explore further any of the avenues discussed above, but will await your directions before going further.

Regarding GL's hands on activity with this payload, it might be possible to set up the existing UVCA payload in the GPIM laboratory and measure the overall spatial resolution using your vacuum tank's collimator to feed the telescope near UV light. The fact that the payload is too big to fit inside the vacuum tank can be circumvented by using a wavelength that does not require a vacuum. The frame grabber and IBM/AT software used with the GL UV Imager could digitize the UVCA analog video and display the point spread function. This activity would provide interesting data and help satisfy your managements desire to have GL take a more active role in the hardware/testing aspects of the UVCA payload.

Regarding a suggestion to improve the UVCA's spatial resolution by replacing the UV sensitive MCP intensifier with a UV sensitive photodiode, the paper Spatial Frequency Response of Proximity Focused Image Tubes in the Near Ultraviolet, SPIE Vol 932. This paper Performance Characteristics of Proximity Focused Ultraviolet Image Converters by Williams and Feibelman, Applied Optics Vol 12, No. 12, page 2832, reports, in Figure 6, experimental data on the MTF of this type of image tube.

The MTF at 10 cycles per mm ranges from 12 to 35 % depending on the wavelength. This is comparable to the estimate I made of the existing MCP tube MTF, indicating perhaps that I was too generous. Based on our own test data reported in this paper, I believe that the MTF of the Ultraviolet sensitive MCP tube is dominated by the MTF of the proximity focus between the photocathode and MCP input face. Removing the MCP will improve the tube's MTF somewhat but from the data in Figure 6, one concludes that the MTF would still be relatively low and the UVCA, with this modification, would still fall far short of the desired spatial frequency response.

10. SUMMARY

The research carried out under this three year contract covered a variety of subjects related to imaging in the ultraviolet and visible wavelength bands. The design study of a high spatial resolution camera for observing the earth in the UV from orbit resulted in a design that would provide high resolution at low ultraviolet brightness levels. This design study will be useful in future satellite payload designs.

The more recent observations of the ionosphere as a participant in the CRRES program demonstrated the advantages for such observations of a cooled unintensified back illuminated CCD based digital television camera with the capability of binning pixels on chip and selected exposure times of many seconds. These observations also highlighted the importance of observing sites and conditions that afford a low background in the wavelength band of interest.